Journal of Microscopy

Journal of Microscopy, 2014
Received 8 October 2013; accepted 9 April 2014

doi: 10.1111/jmi.12135

In vivo noninvasive measurement of skin autofluorescence biomarkers relate to cardiovascular disease in mice

N. AKBAR*, S. SOKOLOVSKI†, A. DUNAEV†, J.J.F. BELCH*, E. RAFAILOV† & F. KHAN*

**Vascular and Inflammatory Diseases Research Unit, Division of Cardiovascular and Diabetes Medicine, Medical Research Institute, Ninewells Hospital and Medical School, University of Dundee, Dundee, Scotland*

†*Photonics and Nanoscience Group, Division of Physics, The School of Engineering, Physics and Mathematics, University of Dundee, Dundee, Scotland*

Key words. Autofluorescence, biomarkers, cardiovascular disease, noninvasive, skin.

Summary

Background and objective

The formation of reactive oxygen species (ROS) is associated with cardiovascular disease (CVD). High dietary cholesterol can significantly alter the delicate balance between pro-oxidation and antioxidant defences leading to reactive oxygen species formation in the vasculature, without significant structural changes in tissue composition. We aimed to establish a methodology for the noninvasive assessment of skin fluorescent biomarkers in mice.

Materials and methods

C57/black/6 wild-type (WT; $n = 25$) male mice were subdivided to receive normal rodent chow ($n = 11$) or a high cholesterol diet (2% cholesterol; $n = 14$) for 20 weeks. Skin autofluorescence measurements were made on the backs of anaesthetized (1.5–2% isoflurane in oxygen) mice. A laser probe was used to make simultaneous measurements of: collagen, elastin, nicotinamide adenine dinucleotide, pyridoxine, flavins, lipofuscin and β-carotene. Results are expressed as group mean in arbitrary units (AU) ± standard error (SE). Hearts were excised and weighed (mg); cardiac hypertrophy was measured by ratio [heart weight (mg)/bodyweight (g) ± SE]. Student's *t*-test was used for statistical significance analysis ($p \leq 0.05$).

Results

There were no significant differences between cholesterol- and chow-fed animals for collagen (34 ± 5AU vs. chow 34 ± 4 AU, $p = 0.51$) and elastin (66 ± 6 AU vs. chow 82 ± 7 AU, $p = 0.11$). Significant differences were evident for nicotinamide adenine dinucleotide (92 ± 7 AU vs. chow 118 ± 7 AU, $p = 0.01$), pyridoxine (56 ± 4 AU vs. chow 73 ± 4 AU, $p = 0.01$), flavins (44 ± 3 AU vs. chow 57 ± 4 AU, $p = 0.01$), lipofuscin (35 ± 3 AU vs. chow 46 ± 3 AU, $p = 0.01$) and β-carotene (19 ± 2 AU vs. chow 25 ± 2 AU, $p = 0.01$). Cholesterol-fed animals had significantly heavier hearts (7 ± 0.3 ratio vs. chow 5 ± 0.1 ratio, $p = 0.001$).

Conclusion

Cholesterol feeding induced cardiovascular disease as noted by cardiac hypertrophy in wild-type mice. A reduction was observed in pyridoxine, nicotinamide adenine dinucleotide, flavins, lipofuscin and β-carotene, which are established risk factors for cardiovascular disease. We report no significant changes in structural proteins collagen and elastin, suggesting no generalized tissue restructuring, which might otherwise explain the observed pathological differences.

Introduction

Established lifestyle factors such as smoking, obesity, a sedentary lifestyle and the intake of high dietary cholesterol are associated with the development of cardiovascular disease (CVD) (Mozaffarian *et al.*, 2008; D'Agostino *et al.*, 2013). The role of these factors in the pathogenesis of CVD is attributed in part to the formation of reactive oxygen species (ROS) (Sugamura *et al.*, 2011); this encompasses a plethora of reactive molecules containing oxygen. Previous studies have documented the ability of ROS to disrupt cellular mechanisms relevant to CVD (De Marchi *et al.*, 2013). Under basal conditions ROS formation is regulated in a delicate balance between pro-oxidation and antioxidant defences. Pro-oxidation is an integral part of physiological function, within the cardiovascular system the enzyme endothelial nitric oxide synthase (eNOS) reduces l-arginine to l-citrulline yielding nitric oxide (NO), an endogenous heterodimer fundamental for basal vascular tone. NO promotes calcium flux in vascular smooth muscle cells inducing vasodilatation. ROS formation, in particular superoxide ($.02^{-}$) can quench the release of NO forming the potent radical peroxynitrite (ONO_{2-}). Due to its oxidizing capacity ONO_{2-} can damage a large number of molecules including

Correspondence to: Faisel Khan, Vascular & Inflammatory Diseases Research Unit, Cardiovascular and Diabetes Medicine, Medical Research Institute, Mail Box 1, Ninewells Hospital and Medical School, Dundee, DD1 9SY, Scotland. Tel: + 44-1382-425574; fax: + 44-1382-632333; e-mail: F.khan@dundee.ac.uk

proteins. The loss of NO bioavailability alters vasomotion, promoting vasoconstriction. This shift in vascular tone promotes luminal narrowing, increasing intra-arterial pressures and is associated with cardiac enlargement (hypertrophy) and atherosclerotic plaque formation. This disruption in oxidation quickly saturates levels of antioxidant defences. Most importantly this change in tissue metabolism precedes any morphological changes in tissue composition (structural changes; Whaley-Connnell *et al.*, 2007). Thus the ability to measure early changes in tissue oxidation holds great therapeutic potential to assess disease manifestation before obvious clinical signs such as plaque formation in CVD.

The ability to assess and quantify the oxidative status of tissues is limited and often involves the use of needle biopsies or venepuncture. Noninvasive imaging is routinely used in research and clinical medicine (Mastouri *et al.*, 2010; Belch *et al.*, 2013); we and others have previously shown the effective use of microvascular imaging in the skin microcirculation and its relationship to coronary artery function and underlying CVD (Khan *et al.*, 2008). Recent emphasis has been placed on the noninvasive assessment of advanced glycation end products (AGEs) in diabetes (Ediger *et al.*, 2009). Advanced glycation end products posses the ability to cross link proteins such as those in vascular smooth muscle, reducing agility and promoting arterial stiffening, this in turn has been associated with CVD (McNulty *et al.*, 2007). This further reinstates the use of skin as a prognostic biomarker for underlying pathophysiology. Here we describe a novel optical technique for the noninvasive assessment of CVD biomarkers/endogenous fluorophores in an *in vivo* mouse model relevant to oxidative stress.

Materials and methods

All experiments were carried out under the authority of a Project licence by a Personal Licence holder issued by the UK Home office. Institutional ethical approval was granted before all described procedures.

Male wild-type (WT) C57/black/6 mice were used in this study and housed in groups of up to five. Mice were kept in a room that maintained at a constant temperature of 22°C ± 2°C with a 12-h light/dark cycle. Distilled water and standard rodent chow (SDS R & M No 3Autoclavable) were fed *ad libitum* for the study duration after weaning (21 days of age) unless otherwise stated.

Study design

WT 12-week-old male mice were subdivided to receive standard rodent chow ($n = 11$) or a specifically tailored proatherogenic diet [$n = 14$; TD.01383 diet, Harlan-Teklad (Maddison, WI, U.S.A.); 18% protein rodent chow with added cholesterol, 2% by weight] for 20 weeks. We have previously reported significant elevations in plasma lipids and the onset of microvascular dysfunction using this model (Belch *et al.*, 2013).

Skin autofluorescence

Animals were weighed (g) and anaesthetized (1.5–2% isoflurane in oxygen). Body temperature was maintained at 37°C using an electric heat mat (VetTech, Congleton, Cheshire, U.K.) and an electric probe (VetTech) was inserted into the animal's rectum using lubricant (KY Jelly Johnson & Johnson, New Brunswick, NJ, U.K.) to monitor core temperature. Skin autofluorescence (SAF) measurements were made on the backs of mice using the 'LAKK-M' (SPE 'LAZMA' Ltd., Russia).

LAKK-M characteristics

The LAKK-M is a multifunctional laser noninvasive diagnostic system, developed for tissue research and diagnostics. The system compromises of four different lasers and is equipped with an optical fibre that has eight individual fibres; four fibres serve as receivers for laser radiation and four fibres for secondary radiation from back scatter. The system has four channels tissue reflectance oximetry, laser Doppler flowmetry, pulse oximetry and fluorescence spectroscopy (Rogatkin *et al.*, 2011; Dunaev *et al.*, 2013a,b). In this study fluorescence spectroscopy was used with an ultraviolet wavelength excitation (365 nm) by light-emitting diode for endogenous fluorescence. The diameter of the optical fibre is 2.5 mm with an approximate distance of 0.6 mm between optical fibre cables. The probe power of fluorescence spectroscopy channel in this multifunctional laser noninvasive diagnostic system is 3–4 mW, the separation distance between the source and detector fibres is about 1 mm (Dunaev *et al.*, 2013a,b) and approximate diagnostic volume within tissue is about 1–2 mm^3 (Rogatkin *et al.*, 2010).

To optimize recordings, 24–48 h prior to SAF measurements animals were shaved using an electric shaver [Tip-to-toe (Carmen) Stoke-on-Trent, West-midlands, U.K.] and depilatory lotion (Veet® Slough, Berkshire, U.K.). This allowed close contact with the dermis for the attachment of a fibre optic probe using double-sided adhesive rings (IAD, Moor Instruments, U.K.). The optic probe consisted of a metre-long fibre cable with a 5.5 cm stainless steel probe. An additional flat disc probe with a protruding element allowed insertion of the optic cable, stabilizing the probe for SAF measurements. The disc probe consisted of 10 mm circumference and a 4 mm interior window through which measurements were made. SAF were used in the ultra-violet spectra through insertion of a spectral density filter for measurement of collagen, elastin, nicotinamide adenine dinucleotide (NADH), lipofuscin, pyridoxine, β-carotene and flavins. Wavelengths for the aforementioned biomarkers have previously been described using the LAKK-M system elsewhere (Smirnova *et al.*, 2012; Rogatkin *et al.*, 2013). The peak emission wavelengths used for the measurement of these compounds are as described in Table 1. A typical SAF spectra is shown in Figure 1 without insertion of a spectral filter, 10 simultaneous recordings were made and subsequently

Table 1. Excitation wavelengths (nm) for collagen, elastin, nicotinamide adenine dinucleotide (NADH), flavins, pyridoxine, lipofuscin and β-carotene.

Compound	λ (nm)
Collagen	420
Elastin	450
NADH	490
Pyridoxine	525
Flavins	550
Lipofuscin	570
β-carotene	608

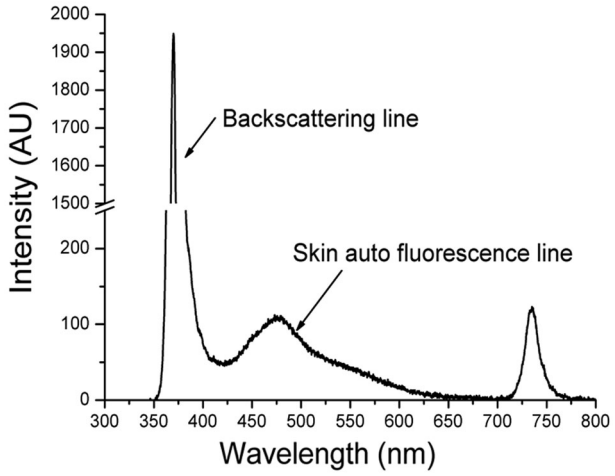

Fig. 1. Typical SAF spectrum (without spectral filter).

averaged; calibration was determined for each individual measurement using the propriety software.

Assessment of CVD

The onset of CVD was determined postmortem. Animals were euthanized by anaesthetic overdose through inhalation of isoflurane preceding cardiac puncture; euthanasia was confirmed by the absence of a respiratory pattern. Animals were perfused with ice cold hepranized (10 units/mL) phosphate buffered saline (20 mL) by insertion of a 23-gauge needle into the left ventricle. Hearts were excised and cleaned of connective and adipose tissue, rolled briefly on gauze to eject any residual blood or phosphate buffered saline and weighed on an electric balance (mg). Ratios were calculated to determine cardiac hypertrophy standardized to body mass [heart weight (mg)/ body weight (g)].

Statistical analysis

SAF results are expressed in arbitrary units (AU) of group mean ± standard error (SE). An unpaired student's *t*-test was used for statistical significance analysis, comparing WT chow- and

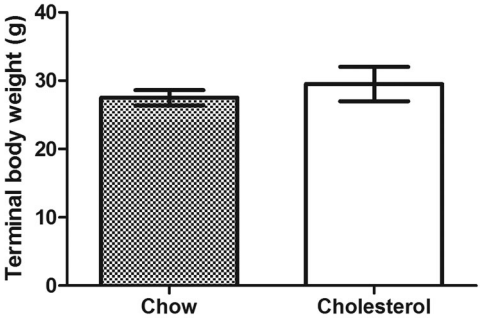

Fig. 2. Terminal body weights for wild-type (WT) chow ($n=11$) and WT cholesterol ($n=14$) fed mice (g ± SE); unpaired t-test.

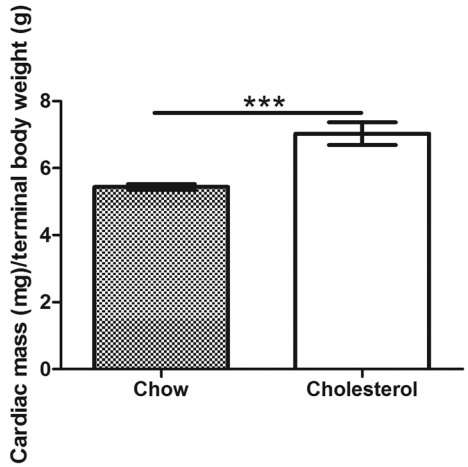

Fig. 3. Cardiac hypertrophy [cardiac mass (mg)/terminal body weight (g) ± SE] for wild-type (WT) chow- ($n = 11$) and WT cholesterol- ($n = 14$) fed mice; unpaired *t*-test.

WT cholesterol-fed mice. The null hypothesis was rejected at $p \leq 0.05$.

Results and discussion

There were no significant differences for terminal body weight between WT chow- (27.5 g ± 1) and WT cholesterol- (29.5 ± 1 g) fed animals ($p = 0.12$; Fig. 2). The onset of CVD was confirmed postmortem by increased cardiac mass equivalent to body mass by ratio (WT cholesterol 7 ± 0.3 ratio vs. WT chow 5 ± 0.1 ratio; $p = 0.001$; Fig. 3). We have previously reported microvascular dysfunction in the skin microvasculature of mice fed a high cholesterol diet, a known cardiovascular risk factor (Belch *et al.*, 2013). The peripheral microvascular network contributes significantly to blood pressure and arterial resistance; peripheral microvascular dysfunction impedes cardiac function as greater force is required to pulsate blood through narrow arteries (the loss of NO bioavailability promotes a vascular phenotype, which is vasoconstricted). Cardiac hypertrophy is thus one mechanism for greater

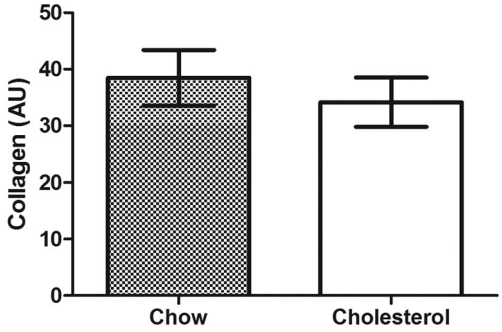

Fig. 4. Skin autofluorescence of collagen in arbitrary units (AU ± SE) for wild-type (WT) chow- ($n = 11$) and WT cholesterol- ($n = 14$) fed mice; unpaired *t*-test.

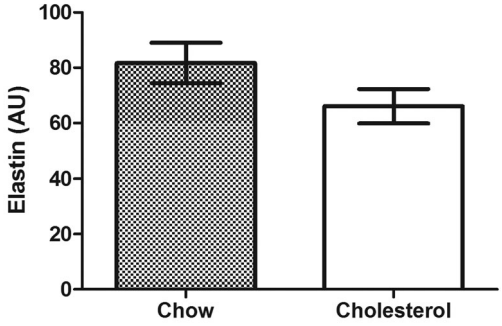

Fig. 5. Skin autofluorescence of elastin in arbitrary units (AU ± SE) for wild-type (WT) chow- ($n = 11$) and WT cholesterol- ($n = 14$) fed mice; unpaired *t*-test.

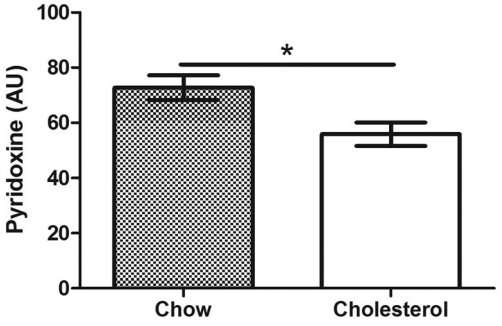

Fig. 6. Skin autofluorescence of pyridoxine in arbitrary units (AU ± SE) for wild-type (WT) chow- ($n = 11$) and WT cholesterol- ($n = 14$) fed mice; unpaired *t*-test.

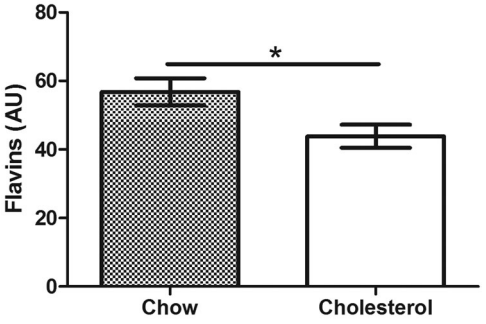

Fig. 7. Skin autofluorescence of flavins in arbitrary units (AU ± SE) for wild-type (WT) chow- ($n = 11$) and WT cholesterol- ($n = 14$) fed mice; unpaired *t*-test.

contractile force through myocyte enlargement, providing greater force for blood ejection from the ventricles (Ledoux *et al.*, 2003).

There were no significant differences between cholesterol- and chow-fed animals for collagen (34 AU ± 5 vs. chow 34 AU ± 4, $p = 0.51$; Fig. 4) and elastin (66 AU ± 6 vs. chow 82 AU ± 7, $p = 0.11$; Fig. 5) suggesting no changes in structural proteins between the two groups. Collagen is a key component of connective tissue and is synthesized in the atherosclerotic process (Cherepanova *et al.*, 2009). Alterations in collagen synthesis (increases in collagen type III and a decrease in collagen I) can cause architectural and functional changes in cardiac tissue leading to diastolic dysfunction (Badenhorst *et al.*, 2003). Another key component of connective tissues is elastin, in blood vessels elastin provides an interface for wave propagation (vasomotion), escalating the pulsation maintaining adequate tissue perfusion. Furthermore elastin significantly contributes to structural shape in many different tissue types. A reduction in elastin has been reported in numerous pathologies including CVD (Grey *et al.*, 2003). The loss of elastin reduces the dexterity of blood vessels and promotes a more constricted vascular phenotype. The similar levels of collagen and elastin in our study may be the result of a mild CVD phenotype. A 2% added cholesterol diet is sufficient enough to cause dyslipidemia with marked endothelial dysfunction, a functional abnormality. However the duration (20 weeks) is not necessarily adequate to cause significant changes in vessel architecture, with immune cell infiltration and robust plaque formation. Late-stage CVD otherwise signifies increases in collagen synthesis and a reduction in elastin (Steed *et al.*, 2010) within vascular tissue. It is possible that with a more aggressive CVD phenotype, more drastic changes in collagen and elastin may be evident, that is, high fat–fed apolipoprotein E (ApoE) knockout animals that are spontaneously dyslipidemic and prone to atherosclerosis.

Under basal conditions numerous antioxidant defences ensure the delicate nature between pro-oxidation and antioxidant defences are maintained. Significant reductions in antioxidants: pyridoxine (56 AU ± 4 vs. chow 73 AU ± 4, $p = 0.01$; Fig. 6), flavins (44 AU ± 3 vs. chow 57 AU ± 4, $p = 0.01$; Fig. 7) and β-carotene (19 AU ± 2 vs. chow 26 AU ± 2, $p = 0.01$; Fig. 8) were observed in WT cholesterol-fed animals when compared with WT chow-fed animals.

Pyridoxine is an established individual risk factor for CVD in humans, better known as vitamin B6. Its role in homocysteine metabolism has been studied extensively, with irregularities in B6 metabolism associated with CVD (Strain

Fig. 8. Skin autofluorescence of β-carotene in arbitrary units (AU $\pm$ SE) for wild-type (WT) chow- ($n = 11$) and WT cholesterol- ($n = 14$) fed mice; unpaired t-test.

Fig. 9. Skin autofluorescence of lipofuscin in arbitrary units (AU $\pm$ SE) for wild-type (WT) chow- ($n = 11$) and WT cholesterol- ($n = 14$) fed mice; unpaired t-test.

et al., 2004). The homocysteine theory was originally postulated by Kilmer McCully (McCully, 2007) in patients with hyperhomocysteinemia who displayed similar vascular insults (lesions). Concluding one or more homocysteine metabolites is harmful to the vasculature. Homocysteine levels are elevated in obesity (Karatela & Sainani, 2009) and in individuals who smoke (O'Callaghan *et al.*, 2002), two established cardiovascular risk factors. Furthermore studies have highlighted the role of B6 in calcium homeostasis in ischemic heart disease, by preventing calcium overload (Dhalla *et al.*, 2013) affirming pyridoxine as a CVD risk factor.

Dietary vitamins remain the largest source of antioxidants in man. Previous studies have highlighted the increased risk of CVD with low serum levels of β-carotene (Karppi *et al.*, 2013). β-carotene is a cell pigment found in many plants and forms the primary source of vitamin A in man. Cell metabolism converts vitamin A to the biological active forms of retinal or retinoic acid. A synthetic retinoic acid (Am80) has shown promising results as a potential future therapy for CVD, with reduced vasculitis and inhibition of neutrophil migration in an animal model (Miyabe *et al.*, 2013), these are early events in the development of CVD.

In addition to the dietary sources of pyridoxine and β-carotene, flavins form important dietary sources of antioxidant defences. Flavins are a class of B vitamins (B2), with important functional roles as coenzymes; riboflavin forms the precursor for biologically active flavins. Tissue distribution of this molecule is broad, however little free riboflavin can be detected. The main coenzyme found is flavin adenine dinucleotide. Flavin adenine dinucleotide is a redox cofactor, with two steady states, electron accepting or donating, for this reason the metabolic activity of the molecule is in oxidative phosphorylation.

As with other antioxidant defences flavins are reported as cardio protective. Tavares *et al.* (2009) found that elderly individuals who were supplemented with riboflavin had reduced plasma homocysteine levels. de Ruijter *et al.* (2009) reported the diagnostic value of homocysteine in a large cohort study where serum levels of homocysteine were better prognostic markers for CVD than traditional measures of cholesterol, smoking or blood pressure.

The current accepted method for quantification of myocardial pathophysiology involves needle biopsies for *ex vivo* scrutiny by histological techniques. This technique, although valuable is limited in application. Samples are only representative of general tissue and are often limited in size to reduce patient discomfort. Nonetheless histological examination of patient biopsies allows semiquantitative analysis to assess pathological status. Routinely myocardial cell number, length, width and collagen deposition may be quantified in CVD; however, the results may be inconclusive and not clinically relevant.

Clinical diagnostic research teams have recently focused on lipofuscin, the so-called 'heart failure' pigment. This cell pigments are readily detected in older patients, however it remains almost absent in children (Strehler *et al.*, 1959). Lipofuscin is the product of phagocytosis, where aged and damaged organelles are processed for destruction by the cell. ROS exposure can significantly hinder this phagocytic process by reducing protease activity, forming ingestible material that can then be detected *ex vivo* in lysosomes (lipofuscin; Parson *et al.*, 2012). Cell pigment molecule lipofuscin (35 AU $\pm$ 3 vs. chow 46 AU $\pm$ 3, $p = 0.01$; Fig. 9) was significantly reduced in cholesterol-fed WT mice when compared to control animals. Previous studies in humans have shown better prognosis (>1 year survival) in patients who suffered a myocardial infarction (MI). Parson *et al.* (2012) reported that those who had higher levels of lipofuscin were able to better respond to cellular stress (oxidative stress). As a result this causes greater accumulation of lipofuscin. The accumulation of lysosomal stores in this fashion is an adequate response to cell damage; whereas an absence of these lysosomal stores would reflect cellular dysfunction and an inability to process cellular material for degradation. In support of this notion, previous studies have not reported a negative association between higher levels of lipofuscin and survival (Parson *et al.*, 2012). We believe this to be the first account showing a relationship between skin levels of lipofuscin and underlying pathology of CVD.

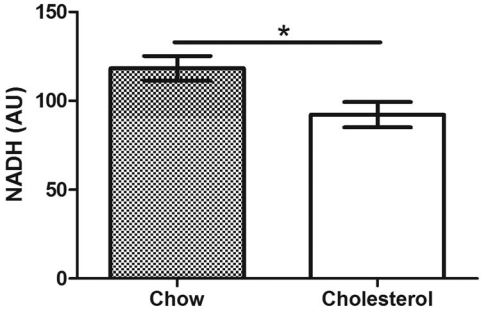

Fig. 10. Skin autofluorescence of nicotinamide adenine dinucleotide in arbitrary units (AU ± SE) for wild-type (WT) chow- ($n = 11$) and WT cholesterol- ($n = 14$) fed mice; unpaired *t*-test.

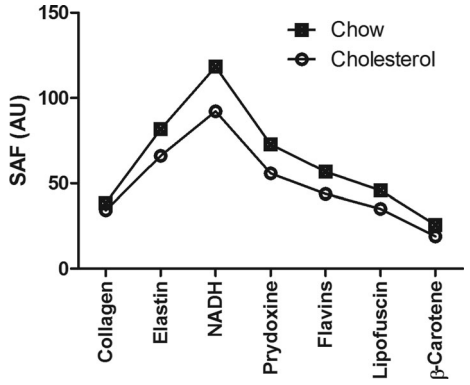

Fig. 11. Averaged skin autofluorescence spectra in arbitrary units (AU) for wild-type (WT) chow- ($n = 11$) and WT cholesterol- ($n = 14$) fed mice showing measurements for collagen, elastin, nicotinamide adenine dinucleotide, flavins, pyridoxine, lipofuscin and β-carotene.

We additionally analysed NADH (92 AU ± 7 vs. chow 118 AU ± 7, $p = 0.01$; Fig. 10) a powerful coenzyme form of the antioxidant vitamin B3. The role of NADH in cellular activity and energy production makes it an important measurement for cell metabolism; a relationship exists between highly active cells (i.e. cardiac myocytes) and high levels of NADH. Here we show reduced levels of NADH in the skin of cholesterol-fed mice; previous studies have effectively shown the important role of NADH in blood pressure and lipid metabolism in an animal model of hypertension. Exogenous NADH effectively reduced blood pressure and total plasma cholesterol when compared to placebo (Bushehri *et al.*, 1998).

Other imaging modalities have been successfully utilized *in vivo* to detect NADH in numerous pathologies. The *in vivo* measurement of NADH by optical methods is notoriously difficult; the excitation of NADH and peak emission is saturated by haemoglobin, which has a very similar excitation/emission spectrum (Mokry *et al.*, 2007); however, we report no clear obstruction in our findings.

Figure 11 shows the averaged SAF measurements obtained from the two groups of WT animals (chow vs. cholesterol). The spectral shape appears similar between the experimental groups, concluding that the differences observed in the peak emission maxima were due to differences in fluorescence intensity and not a significant change in the emission spectrum.

The role of cholesterol in CVD (Belch *et al.*, 2013) is well established. Under basal physiological conditions plasma lipids are maintained within strict thresholds; the intake of dietary cholesterol and cholesterol efflux are tightly regulated to ensure this homeostasis is maintained. Increased cholesterol consumption elevates plasma levels by outstripping efflux. This higher titre level of circulating plasma lipids interfaces with a number of host tissues, including those with reduced antioxidant defences and increased oxidative stress. Plasma lipids can readily become oxidized; in particular, the oxidation of the low-density lipoproteins is associated with atherogenic lesion formation. Oxidation of the low-density lipoproteins is taken up by tissue macrophages and accumulates in these cells, forming the characteristic atherogenic foam cell. A cycle of inflammation perpetuates the infiltration of monocytes which mature into tissue macrophages, up taking oxidation of the low-density lipoproteins and contributing to the developing vascular lesion. Numerous studies have established the potential role of antioxidant replacement therapy in reducing CVD prevalence, with increased circulating levels of antioxidant defences and reduced oxidation of the low-density lipoproteins (Ruel *et al.*, 2005). Furthermore studies have highlighted the improvement of CVD risk after antioxidants in humans (Galleano *et al.*, 2009).

Conclusions

Here we report the noninvasive assessment of established CVD biomarkers in an *in vivo* mouse model, the skin served as a surrogate biomarker for underlying pathology. Although no significant differences were observed for structural proteins, we report a significant reduction in antioxidant defences, suggestive of altered homeostasis of tissue oxidation. The LAKK-M may provide a novel tool for the assessment of tissue oxidation in pathological processes.

Conflicts of interest

The authors report no conflicts of interest.

References

Badenhorst, D., Maseko, M., Tsotetsi, O.J., Naidoo, A., Brooksbank, R., Norton, G.R. & Woodiwiss, A.J. (2003) Cross-linking influences the impact of quantitative changes in myocardial collagen on cardiac stiffness and remodelling in hypertension in rats. *Cardiovasc Res.* **57**, 632–641.

Belch, J.J., Akbar, N., Alapati, V., Petrie, J., Arthur, S. & Khan, F. (2013) Longitudinal assessment of endothelial function in the microvasculature of mice in-vivo. *Microvasc Res.* **85**, 86–92.

Bushehri, N., Jarrell, S.T., Lieberman, S., Mirdamadi-Zonozi, N., Birkmayer, G. & Preuss, H.G. (1998) Oral reduced B-nicotinamide adenine dinucleotide (NADH) affects blood pressure, lipid peroxidation, and lipid profile in hypertensive rats (SHR). *Geriatr. Nephrol. Urol.* **8**, 95–100.

Cherepanova, O.A., Pidkovka, N.A., Sarmento, O.F., *et al.* (2009) Oxidized phospholipids induce type VIII collagen expression and vascular smooth muscle cell migration. *Circ. Res.* **104**, 609–618.

D'Agostino, R.B., Sr., Pencina, M.J., Massaro, J.M. & Coady, S. (2013) Cardiovascular disease risk assessment: insights from framingham. *Glob. Heart* **8**, 11–23.

De Marchi, E., Baldassari, F., Bononi, A., Wieckowski, M.R. & Pinton, P. (2013) Oxidative stress in cardiovascular diseases and obesity: role of p66Shc and protein kinase C. *Oxid. Med. Cell. Longev.* **2013**, 1–11.

Dhalla, N.S., Takeda, S. & Elimban, V. (2013) Mechanisms of the beneficial effects of vitamin B6 and pyridoxal 5-phosphate on cardiac performance in ischemic heart disease. *Clin. Chem. Lab. Med.* **51**, 535–543.

Dunaev, A.V., Sidorov, V.V., Stewart, N.A., Sokolovski, S.G. & Rafailov, E.U. (2013a) Laser reflectance oximetry and Doppler flowmetry in assessment of complex physiological parameters of cutaneous blood microcirculation. In *Proceedings SPIE 8572, Advanced Biomedical and Clinical Diagnostic Systems XI* (eds. A. Mahadevan-Jansen, T. Vo-Dinh, & W.S. Grundfest), 857205. San Francisco, USA.

Dunaev, A.V., Zherebtsov, E.A., Rogatkin, D.A., Stewart, N.A., Sokolovski, S.G. & Rafailov, E.U. (2013b) Substantiation of medical and technical requirements for noninvasive spectrophotometric diagnostic devices. *J. Biomed. Opt.* **18**, 107009.

Ediger, M.N., Olson, B.P. & Maynard, J.D. (2009) Noninvasive optical screening for diabetes. *J. Diabetes Sci. Techno.* **3**, 776–780.

Galleano, M., Oteiza, P.I. & Fraga, C.G. (2009) Cocoa, chocolate, and cardiovascular disease. *J Cardiovasc. Pharmacol.* **54**, 483–490.

Grey, E., Bratteli, C., Glasser, S.P., Alinder, C., Finkelstein, S.M., Lindgren, B.R. & Cohn, J.N. (2003) Reduced small artery but not large artery elasticity is an independent risk marker for cardiovascular events. *Am. J. Hypertens.* **16**, 265–269.

Karatela, R.A. & Sainani, G.S. (2009) Plasma homocysteine in obese, overweight and normal weight hypertensives and normotensives. *Indian Heart J.* **61**, 156–159.

Karppi, J., Kurl, S., Ronkainen, K., Kauhanen, J. & Laukkanen, J.A. (2013) Serum carotenoids reduce progression of early atherosclerosis in the carotid artery wall among Eastern Finnish men. *PLoS One* **8**, e64107.

Khan, F., Patterson, D., Belch, J.J., Hirata, K. & Lang, C.C. (2008) Relationship between peripheral and coronary function using laser Doppler imaging and transthoracic echocardiography. *Clin. Sci. (Lond.)* **115**, 295–300.

Ledoux, J., Gee, D.M. & Leblanc, N. (2003) Increased peripheral resistance in heart failure: new evidence suggests an alteration in vascular smooth muscle function. *Br. J. Pharmacol.* **139**, 1245–1248.

Mastouri, R., Sawada, S.G. & Mahenthiran, J. (2010) Current noninvasive imaging techniques for detection of coronary artery disease. *Expert Rev. Cardiovasc. Ther.* **8**, 77–91.

McCully, K.S. (2007) Homocysteine, vitamins, and vascular disease prevention. *Am. J. Clin. Nutr.* **86**, 1563S–1568S.

McNulty, M., Mahmud, A. & Feely, J. (2007) Advanced glycation endproducts and arterial stiffness in hypertension. *Am. J. Hypertens.* **20**, 242–247.

Miyabe, C., Miyabe, Y., Miura, N.N., *et al.* (2013) Am80, a retinoic acid receptor agonist, ameliorates murine vasculitis through the suppression of neutrophil migration and activation. *Arthritis Rheu.* **65**, 503–512.

Mokry, M., Gal, P., Harakalova, M., Hutnanova, Z., Kusnir, J., Mozes, S. & Sabo, J. (2007) Experimental study on predicting skin flap necrosis by fluorescence in the FAD and NADH bands during surgery. *Photochem. Photobiol.* **83**, 1193–1196.

Mozaffarian, D., Wilson, P.W. & Kannel, W.B. (2008) Beyond established and novel risk factors: lifestyle risk factors for cardiovascular disease. *Circulation* **117**, 3031–3038.

O'Callaghan, P., Meleady, R., Fitzgerald, T. & Graham, I. (2002) Smoking and plasma homocysteine. *Eur. Heart J.* **23**, 1580–1586.

Parson, S.J., Russell, S.D., Bennett, M.K., *et al.* (2012) Increased lipofuscin on endomyocardial biopsy predicts greater cardiac improvement in adolescents and young adults. *Cardiovasc. Pathol.* **21**, 317–323.

Rogatkin, D.A. & Smirnova, O.D. (2013) Mathematical modelling of signals recorded in noninvasive medical laser fluorescence diagnosis. *J. Optic. Technol.* **80**, 566–570.

Rogatkin, D.A., Dunaev, A.V. & Lapaeva, L.G. (2010) Metrological support of methods and devices for noninvasive medical spectrophotometry. *Biomed. Eng.* **44**, 66–70.

Rogatkin, D.A., Sokolovski, S.G., Fedorova, K.A., Sidorov, V.V., Stewart, N.A. & Rafailov, E.U. (2011) Basic principles of design and functioning of multifunctional laser diagnostic system for non-invasive medical spectrophotometry. In *Proceedings SPIE 7890, Advanced Biomedical and Clinical Diagnostic Systems IX* (eds. A. Mahadevan-Jansen, T. Vo-Dinh & W.S. Grundfest), 78901H. San Francisco, USA.

Ruel, G., Pomerleau, S., Couture, P., Lamarche, B. & Couillard, C. (2005) Changes in plasma antioxidant capacity and oxidized low-density lipoprotein levels in men after short-term cranberry juice consumption. *Metabol.-Clin. Experiment.* **54**, 856–861.

de Ruijter, W., Westendorp, R.G., Assendelft, W.J., den Elzen, W.P., de Craen, A.J., le Cessie, S. & Gussekloo, J. (2009) Use of Framingham risk score and new biomarkers to predict cardiovascular mortality in older people: population based observational cohort study. *BMJ* **338**, 1–8.

Smirnova, O.D., Rogatkin, D.A. & Litvinova, K.S. (2012) Collagen as in vivo quantitative fluorescent biomarkers of abnormal tissue changes. *J. Innov. Opt. Health Sci.* **5**, 1–9.

Steed, M.M., Tyagi, N., Sen, U., Schuschke, D.A., Joshua, I.G. & Tyagi, S.C. (2010) Functional consequences of the collagen/elastin switch in vascular remodeling in hyperhomocysteinemic wild-type, eNOS-/-, and iNOS-/- mice. *Am. J. Physiol. Lung Cell. Mol. Physiol.* **299**, L301–311.

Strain, J.J., Dowey, L., Ward, M., Pentieva, K. & McNulty, H. (2004) B-vitamins, homocysteine metabolism and CVD. *Proc. Nutr. Soc.* **63**, 597–603.

Strehler, B.L., Mark, D.D. & Mildvan, A.S. (1959) GEE MV: rate and magnitude of age pigment accumulation in the human myocardium. *J. Geronto.* **14**, 430–439.

Sugamura, K. & Keaney, J.F., Jr. (2011) Reactive oxygen species in cardiovascular disease. *Free Radic. Biol. Med.* **51**, 978–992.

Tavares, N.R., Moreira, P.A. & Amaral, T.F. (2009) Riboflavin supplementation and biomarkers of cardiovascular disease in the elderly. *J. Nutr. Health Ag.* **13**, 441–446.

Whaley-Connell, A., Govindarajan, G., Habibi, J., et al. (2007) Angiotensin II-mediated oxidative stress promotes myocardial tissue remodeling in the transgenic (mRen2) 27 Ren2 rat. *Am. J. Physiol. Endocrinol. Metab.* **293**, E355–363.